PPPL-3149 - Preprint Date: December 1995, UC-420, 426

Ballooning Instability Precursors to High β Disruptions

E. D. Fredrickson, K. M. McGuire, Z. Y. Chang, A. Janos, J. Manickam, G. Taylor
Plasma Physics Laboratory, Princeton University
P.O. Box 451, Princeton, New Jersey, 08540 USA

S. Mirnov, I. Semenov
TRINITI, Moscow Reg., USSR

D. Kislov, D. Martynov
RRC Kurchatov Institute, Moscow, Russia

Abstract

Strongly ballooning modes have been found as precursors to high β disruptions on TFTR. The modes are typically localized to a region spanning about 60º in the toroidal direction. The toroidal localization is associated with lower frequency, global Magneto-Hydro-Dynamic (MHD) activity, typically an ideal n=1 kink mode. They have moderate to high frequency (f = 10-20 f_{rot}), implying toroidal mode numbers in the range n = 10-20. The growth rates for the modes are large, of order 10^4/sec.

Introduction

Attempts to increase the stored energy indefinitely in plasmas, with fixed plasma current and toroidal field, result in disruptions. This limit on the amount of stored energy which a plasma with given external parameters can hold can be characterized as a β limit, i.e., a limit on the ratio of kinetic to magnetic energy in a plasma. Empirically, the β limit on TFTR appears to follow the high n-ballooning stability criterion. The empirical stability limit for TFTR is not well characterized by the Troyon limit [1], i.e., the maximum $\beta_{Tor} \propto \beta_{Troyon}$ [$\beta_{Troyon} \equiv Ip(MA)/a(m)B_{Tor}(T)$]. but requires the inclusion of terms related to the pressure peakedness[2,3], Developing a better understanding of this constraint on plasma performance is of critical importance to the future of the fusion program.

Studies of the precursors to β limit disruptions on TFTR [4-7] have resulted in the general model that the disruptions are the result of a combination of a low n global MHD mode and a toroidally localized ballooning mode. In many cases a clear, high frequency mode with inferred toroidal mode numbers in the range 10-20 and ballooning characteristics has been observed to be strongly growing just prior to β-limit disruptions. The high frequency modes are apparently localized in toroidal angle by the presence of n=1 MHD activity. In this paper the range of ballooning mode activity, details of the experimental data and analysis and scaling of the growth rate and toroidal mode numbers will be presented.

General discussion

The disruption precursor modes are studied with the array of fast MHD diagnostics. While the full set of MHD diagnostics are not available for all disruptions, they include; a 30 channel, Mirnov coil system, a 59 channel, horizontally viewing soft x-ray camera and a 20 channel vertically viewing soft x-ray camera, a multi-channel, plastic scintillator system for fast measurements of the neutron emission, fast measurements of the escaping fusion products (α's from D-T reactions and tritons from D-D reactions), fast measurements of the Hα and CII emission, fast measurements of the bumper limiter surface temperature and two 20 channel electron cyclotron emission (ECE) grating polychromators (GPC's). These diagnostics typically have bandwidths of order or greater than 200kHz and are synchronously digitized at rates up to 500kHz. A significant fraction of disruptions are captured through the use of a trigger generated by the rise in the limiter surface temperature and the pre-trigger capability in the digitizers. The addition of the second GPC, toroidally separated from the first by 126°, has provided confirming evidence of the toroidal localization of the ballooning mode.

The ballooning modes are visible only on the two GPC's, not on either the Mirnov system or on the soft x-ray camera. This is probably due to a relatively high toroidal wave number and, presumably, high poloidal mode number. The soft x-ray camera measures the chord integrated emissivity, thus the high n and m would cause a relatively small fluctuation level in the chord integrated data. In simulations using an assumed structure for the ballooning modes, the soft x-ray fluctuation level, as a fraction of the equilibrium level, was about 10% of the local electron temperature fluctuation level. Likewise, the magnetic perturbation from the mode will fall off with minor radius approximately as $(r/r_s)^{m+1}$ and is also expected to be weak at the plasma edge. The lack of Mirnov data on the ballooning modes is particularly unfortunate as it precludes direct measurements of the toroidal mode numbers.

Disruptions in high performance supershot regime plasmas are relatively infrequent on TFTR due to the reproducible nature of the plasmas and the well defined empirical β limits. Thus, in the early 1994 campaign only five high β major disruptions were made, including two in plasmas with approximately equal injection of Deuterium and Tritium beams. In the later part of the 1994 campaign and into 1995, more exotic regimes of operation were systematically explored, resulting in additional disruptions. Of the (≈20) disruptions included in this study, (≈10) have clearly identifiable ballooning precursors. Disruptions for which ballooning mode precursors have been identified have occurred in standard supershot regime plasmas, high β plasmas where the current profile is modified through current ramps[8], and in enhanced reversed shear plasmas[9].

Description of mode

In Figure 1a and 1b are shown plots of the contours of constant electron temperature, from GPC1 in Figure 1a and from GPC2 in Figure 1b. The relative locations of the GPC's are indicated in the small cartoon as is the direction of the rotation of the plasma (which is in the ω_{*e} direction). The toroidal localization is suggested in figure 1a from the "bursting" character of the mode, as well as the synchronization of the bursts with the global MHD (in this case an m=1, n=1 kink mode). The data are clearly not consistent with a global mode which bursts in time, as the bursts do not appear simultaneously on the two diagnostics (Fig. 1b). The timing of the bursts between the two diagnostics is consistent, however, with a toroidally localized mode rotating in the plasma frame. The slower oscillations of the contours are the n=1 kink mode, and an approximate phase delay of 120° is seen between the GPC1 and GPC2 data. The ballooning mode is localized to the toroidal region where the kink pushes the plasma towards the weak field side of the machine.

The ballooning character of the mode can be seen in the measurements of the electron temperature. In the disruptions where the GPC data covered the inboard and outboard locations of the ballooning mode, the mode was not visible or much weaker on the inboard side of the plasma. In Figs. 2a and 2b the ballooning mode is clearly visible as multiple bursts on the outboard side. There is no visible activity on the inboard side. GPC data is not always available over the entire profile on each shot, and the ballooning character of the modes is inferred from a limited sample.

The toroidal extent of the mode may be inferred from the figure where each full slow oscillation corresponds to one full 360° rotation toroidally. (The toroidal mode number of the slow oscillation is measured to be unity with the Mirnov array.) In the example shown in Figure 1, the ballooning mode oscillations span about 1/4 of the n=1 kink period, thus in this case they span about 90° in the toroidal direction. It might be expected that the smaller the amplitude of the n=1 kink, the less toroidally localized the ballooning mode would become. That is in the limit that the plasma globally reached the ballooning threshold in the absence of the symmetry breaking n=1 kink, the ballooning mode should be global. This is supported in the data. In Figure 3 is shown data preceding a minor disruption under very similar plasma conditions as in Figure 1. In this second example, the n=1 mode was not discernible in the GPC data. An n=1 mode was observed in the Mirnov data at an initial amplitude approximately 20% of the precursor amplitude in shot 76778 (Fig. 1). This level would be consistent with the mode not being observable with the GPC's, assuming a linear relationship between the local mode amplitude as measured by the GPC and the Mirnov diagnostics. The toroidal localization of the mode is in this case much weaker, suggesting that the presence of the global MHD is important for the initial toroidal localization. Closer to the time of the first thermal quench, the n=1 mode becomes stronger (both in the Mirnov data and now in the GPC data) and the ballooning mode becomes more toroidally localized. The increased toroidal localization is also predicted by the numerical simulations of Park[7].

Using data from the two GPC's, the displacement of the flux surface associated with the ballooning mode, as inferred from the shifts in the temperature contours can be measured. In Figure 4 is shown the radial profile of the peak of this displacement in each 'burst' seen by the GPC's leading to the disruption. The ballooning modes during their early growth phase are localized to a region of about 0.2m or about 20% of the minor radius. The radial extent of the mode increases as it grows in amplitude, and there is some suggestion that the peak of the mode amplitude shifts to larger minor radius. The growth time of the mode is about 50 μsec, compared with, for example, the Alfvén time of about 0.1 μsec.

Direct measurement of the toroidal mode number of the ballooning modes is not possible with the present diagnostic set. Only in cases where the modes are measurable on the Mirnov system is it possible to unambiguously determine the toroidal mode number, n. The toroidal mode number can be inferred from the relative frequency of the n=1 kink mode and the ballooning mode. This analysis presumes that the real frequency of the mode in the plasma frame (the rest frame of the n=1 mode) much less than observed ballooning mode frequency and is thus somewhat questionable.

The ballooning mode is most commonly observed in the presence of a fast growing n=1 kink mode. The amplitude of this kink at the time of the disruption can vary substantially, but in general the amplitude is smaller than the similar fishbone-like n=1 kink [10] commonly observed in non-disruptive plasmas (Figure 5). It is believed that the n=1 kink plays the secondary role in the disruption of locally triggering the ballooning mode as suggested by Hegna and Callen [11]. Thus, it might be presumed that the amplitude of the n=1 kink necessary to trigger the ballooning mode would decrease as the plasma approaches the ballooning mode threshold. This presumption is somewhat supported in calculations of the ballooning stability margin for two disruptions with large and small kinks. However, the uncertainties in the calculated current and pressure profiles make this analysis suggestive at best.

Discussion

The conclusion that the global MHD activity plays a lesser role in the disruption is supported by an example in which the plasma disrupted in the presence of an (m,n)=(4,3) mode. In this case the ballooning mode activity was also observed, however, it was now toroidally localized by the n=3 mode. Most interestingly, the ballooning mode was still localized to only one toroidal location, i.e., only one of three oscillations of the toroidally rotating n=3 mode showed evidence of the ballooning mode activity. This example is the strongest evidence yet that the ballooning mode plays an important role in the disruption process. In the example in Figure 6, in which the background MHD activity was an (m,n)=(4,3) mode, the toroidal extent is only about 30º to 40º. While due to the limited amount of experimental data, these observations are anecdotal, they do support the conjecture that the n=1 mode plays little direct role in the disruption, and that the main contribution of this mode is to toroidally localize them and de-stabilize the ballooning modes somewhat earlier than they would have naturally. It must be pointed out that there as yet no examples of disruptions which happened in the absence of any detectable global, low n precursor, although in many cases this precursor was very weak (e.g., Figure 3).

The initial partial thermal quench may directly result from the non-linear evolution of the ballooning modes. At large enough amplitude they would locally break the closed flux surfaces allowing rapid parallel transport of heat to the plasma edge. It is also possible that the ballooning modes either directly or indirectly destabilize fast growing global MHD modes. During this stage of the disruption the grating polychromators are typically blinded by a large burst of non-thermal electron cyclotron emission and the MHD activity must be inferred from other diagnostics[12].

The sequence of events leading to the minor disruption is then as follows. The plasma is heated to near the ballooning stability boundary. In the presence of a low n, global MHD mode, the plasma locally (in the toroidal direction) exceeds the ballooning stability threshold. If the plasma is near the ballooning threshold over much of the minor radius, the ballooning mode can continue to grow non-linearly until the edge of the plasma is reached. The locally stochastic region created by the ballooning mode causes a partial thermal quench of the plasma; the transient increase in heat flux to the limiter liberates impurities which trigger a slower thermal collapse leading to the major disruption. If the plasma is only near the ballooning threshold over a small part of the minor radius, the ballooning modes cause just a small thermal quench of the plasma. The heat deposition on the limiter is not sufficient to trigger a large enough impurity influx to lead to a major disruption. However, the local tearing of the flux surfaces does allow non-linear growth of tearing modes as predicted by the neo-classical theory [13]. The presence of these modes results in substantial degradation of plasma performance, as has been previously documented [14].

The ballooning modes described in this paper should not be confused with the more ubiquitous high frequency modes (KBM-like modes) commonly seen in high β plasmas on TFTR [15,16]. These KBM-like modes are visible on the Mirnov and soft x-ray diagnostics, implying lower toroidal mode numbers. They are believed to be directly associated with disruptive events.

Summary

In this paper is presented detailed data on ballooning precursors to b-limit disruptions. This data presents the strongest argument that the β-limit in tokamaks is set by moderate n ballooning modes as in the model proposed by Hegna and Callen and the simulations by Park.

While these modes are extremely difficult to study, as they are visible on only a few diagnostics and for a short time prior to disruptions, a fairly clear picture of their role in the disruption has emerged. As the ballooning limit is approached, the presence of low n MHD activity can push the plasma over the stability boundary in a toroidally localized region. The ballooning modes grow rapidly. As they grow, they distort the plasma in an ever growing region until the distortion reaches the edge of the plasma. As the ballooning modes are very local, having large gradients within them, they can drive flux reconnection on a timescale much faster than the global tearing mode timescale, creating a locally stochastic region. This results in the initial thermal quench of the plasma, initiating events leading to the final major disruption.

ACKNOWLEDGMENTS

We would like to thank Drs. K. Young and R. Hawryluk and the TFTR group for supporting these experiments. Supported by the U.S. Department of Energy Contract Number DE-AC02-76CH03073.

Bibliography

[1] F. Troyon, R Gruber, H Saurenmann, S Semenzato, S Succi, Plasma Physics and Controlled Fusion **26**, 209, 1984.

[2] J. Manickam, V. Arunasalem, C. W. Barnes, M. Bell, M. Bitter, H. S. Bosch, N. L. Bretz, R. V. Budny, C. Bush, A. Cavallo, L. Chen, C Z. Cheng, T. K . Chu, S. A. Cohen, P. Colestock, D. Coster, D. L. Dimock, H. F. Dylla, P. C. Efthimion, A. Ehrhardt, R. J. Fonck, E. D. Fredrickson, H. P. Furth, G. Gammel, R. J. Goldston, G. Greene, B. Grek, L. Grisham, G. Hammet, R. J. Hawryluk, H. W. Hendel, K Hill, E. Hinnov, S. P. Hirshman, J. Hosea, B. Howell, H. Hsuan, R. Hulse, A. C. Janos, D. Jassby, D. Johnson, R. Kaita, S. Kieras-Phillips, S. J. Kilpatrick, V. A. Krupin, P. H. LaMarche, B. LeBlanc, R. Little, A. I. Lysoyvan, D. M. Manos, D. Mansfield, E. Mazzucato, D. McCarthy, D. C. McCune, K.M. McGuire, D. H. McNeill, D. Meade, D. R. Mickelsen, A. D. Monticello, R. Motley, S. S. Medley, D. Mueller, J. Murphy, Y. Murakami, D. K. Owens, H. K. Park, W. Park, A. Ramsey, M. H. Redi, T. Saito, G. Schilling, J. Schivell, G. L Schmidt, S. D. Scott, J. C. Sinnis, B. C. Stratton, W. Stodiek, E. J. Synakowski, G. Taylor, H. H. Towner, M. Ulrickson, S. von Goeler, R. M .Weiland, R. White, J. R. Wilson, K. M Young, M .C. Zarnstorf and S. Zweben, in Plasma Physics and Controlled Nuclear Fusion Research 1988 (Proc. 12th Int. Conf. Nice, 1988). Vienna (1989) .

[3] D. Mueller, M. G. Bell, E. Fredrickson, Bull. Am. Phys. Soc. **39** 1671 (1994) (submitted to

Fusion Technology, June 1995)
[4] K. M. McGuire, E. Fredrickson, Phys. of Plasmas **2** 2176 (1995)
[5] E Fredrickson, S Batha, M Bell, R Budny, C Bush, Z Chang, C Z Cheng, D S Darrow, J.Dunlap, G Y Fu, H W Herrmann, H Hsuan, R Majeski, D K Mansfield, E Mazzucato, K M McGuire, D R Mikkelsen, M Murakami, R Nazikian, A Janos, C K Phillips, S A Sabbagh, G L Schmidt, S D Scott, J D Strachan, E Synakowski, H Takahashi, G Taylor, J R Wilson, K L Wong, M C Zarnstorff, S Zweben and the TFTR Group, to be published in Plasma Physics and Controlled Nuclear Fusion Research 1995 (Proc. 15th Int. Conf. Sevilla, Spain, 1995) Vienna (1995) .
[6] E. D. Fredrickson, K. McGuire, Z. Chang, A. Janos, M. Bell, R. V. Budny, C. E. Bush, J. Manickam, H. Mynick, R. Nazikian, G. Taylor, Phys. of Plasmas **2** (1995).
[7] W. Park, E.D. Fredrickson, A. Janos, J. Manickam, W.M. Tang Phys. Rev. Lett. **75**, 1763 (1995).
[8] S A Sabbagh,, R A Gross, M E Mauel, G A Navratil, M G Bell, E D Fredrickson, R Hatcher, R J Hawryluk, S P Hirschman, A C Janos, S C Jardin, D L Jassby, J Manickam, D C McCune, K M McGuire, S S Medley, D Mueller, Y Nagayama, D K Owens, M Okabayashi, H K Park, A T Ramsey, B C Stratton, E J Synakowski, G Taylor, R M Wieland, M Zarnstorff, J Kesner, E S Marmar, and J Terry, Phys. Fluids B **3**, 2277 (1991).
[9] F. Levinton, M C Zarnstorff, S H Batha, M G Bell, R E Bell, R V Budny, C Bush, Z Chang, E D Fredrickson, A C Janos, H K Park, A T Ramsey, G L Schmidt, E Synakowski, G Taylor (submitted to Phys. Rev. Lett.)
[10] R.Kaita, R. B. White, A. W. Morris, E. D. Fredrickson, K. McGuire, S. S. Medley, and S. D. Scott, Phys. Fluids B **2**, 1584 (1990).
[11] C. C. Hegna and J. D. Callen, Phys. Fluids B **4**, 3031 (1992).
[12] S. Mirnov, I. Semenov, E. Fredrickson, R. Budny, K. McGuire, H. Park, S. Zweben, L.Zacharov, S. Von Goeler (to be published)
[13] Z. Chang, J. D. Callen, E. Fredrickson, R V Budny, C C Hegna, K M McGuire, M C Zarnstorff, and TFTR Group, Phys. Rev. Lett. **74** (1995) 4663.
[14] Z. Chang, E. Fredrickson, J. D. Callen, K. M. McGuire, Nucl Fusion **34**, 1309 (1994).
[15] Y. Nagayama, M. Yamada, S A Sabbagh, E D Fredrickson, J Manickam, M Bell, R V Budny, A Cavallo, A C Janos, M Mauel, K M McGuire, G A Navratil, Phys. Fluids B **5** 2571 (1993).
[16] R. Nazikian (Submitted to Phys. of Plasmas)

Figure Captions

1 Contour plot of constant electron temperature across the plasma midplane vs. time. Data from the two GPC's, separated by 126° in the toroidal direction is shown. 76778

2 Contour plot of constant electron temperature across the plasma midplane vs. time. Data from the two GPC's, separated by 126° in the toroidal direction is shown. 83546

3 Contour plot of constant electron temperature across the plasma midplane vs. time. Data from the two GPC's, separated by 126° in the toroidal direction is shown. 76773

4 Growth of the ballooning mode prior to a major disruption.

5 Comparison of the amplitudes of typical n=1 'fishbone' oscillations during a non-disruptive plasma and the n=1 precursor to a major disruption.

6 Example of a ballooning mode in the presence of (m=4, n=3) global MHD.

Figure 1

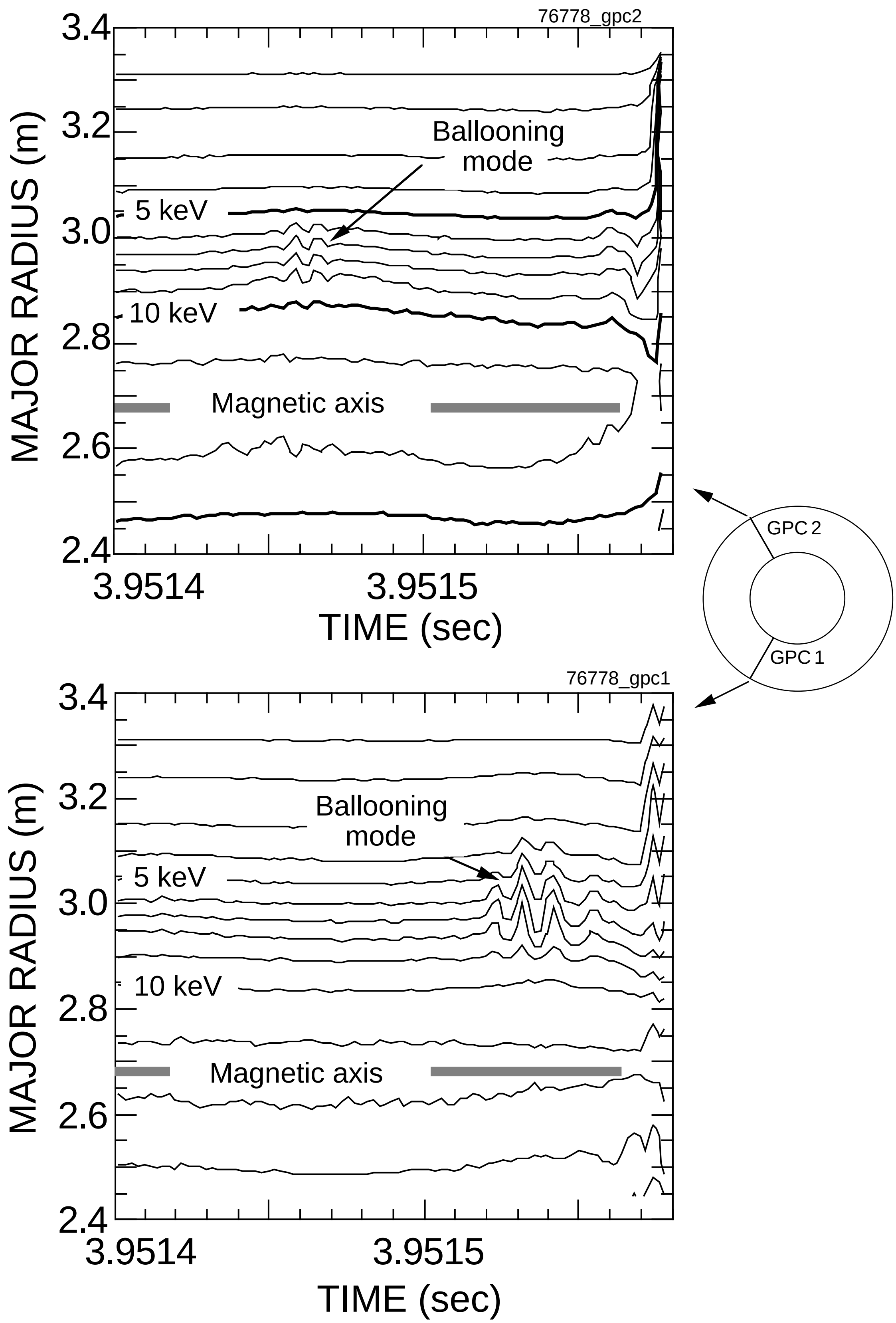
76778_gpc2
3.4
3.2
3.0
2.8
2.6
2.4
MAJOR RADIUS (m)
Ballooning mode
5 keV
10 keV
Magnetic axis
3.9514
3.9515
TIME (sec)
GPC 2
GPC 1
76778_gpc1
3.4
3.2
3.0
2.8
2.6
2.4
MAJOR RADIUS (m)
Ballooning mode
5 keV
10 keV
Magnetic axis
3.9514
3.9515
TIME (sec)

Figure 2

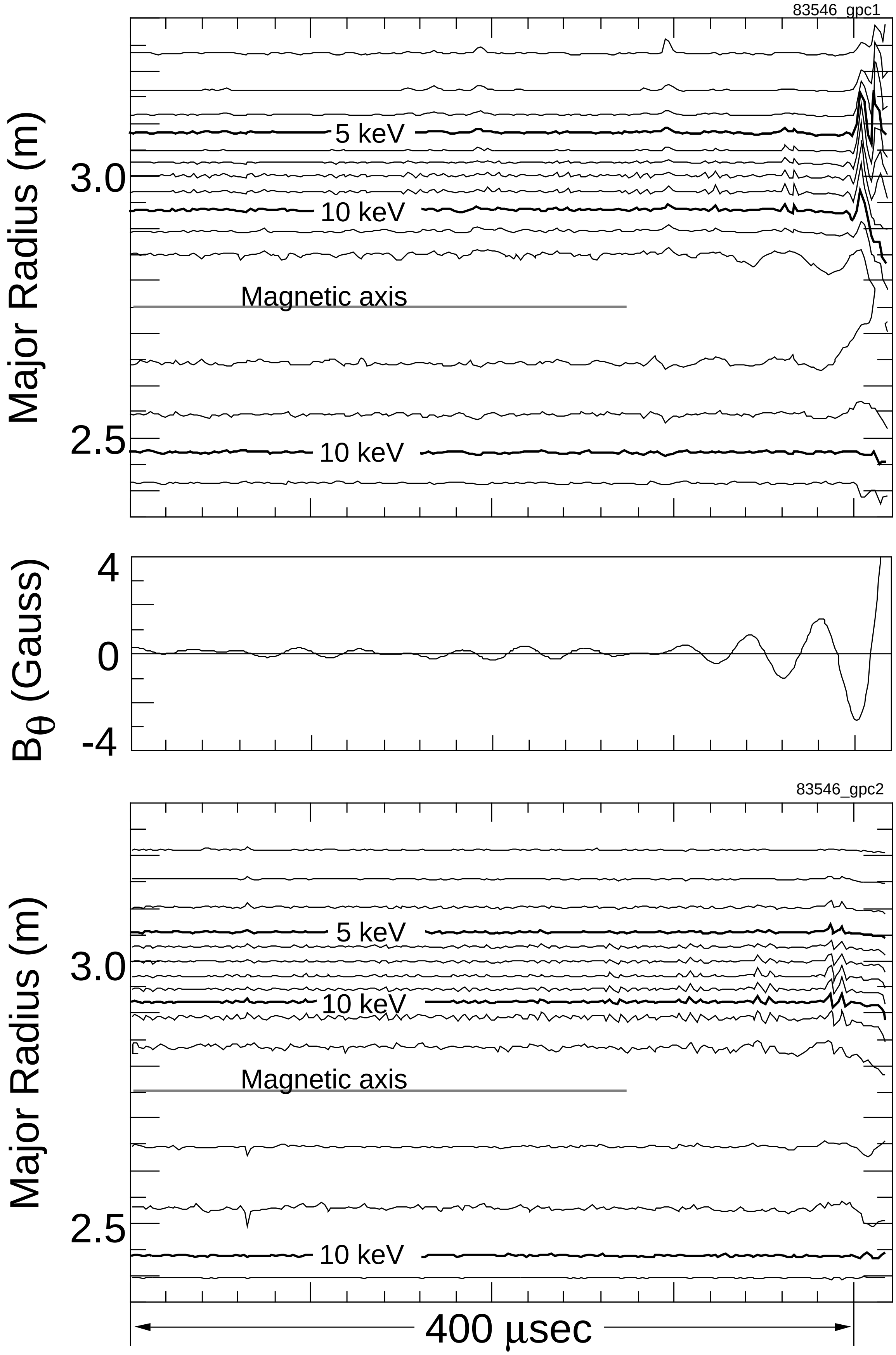
83546_gpc1
Major Radius (m)
3.0
2.5
5 keV
10 keV
Magnetic axis
10 keV
Bθ (Gauss)
4
0
-4
83546_gpc2
Major Radius (m)
3.0
2.5
5 keV
10 keV
Magnetic axis
10 keV
400 μsec

Figure 3

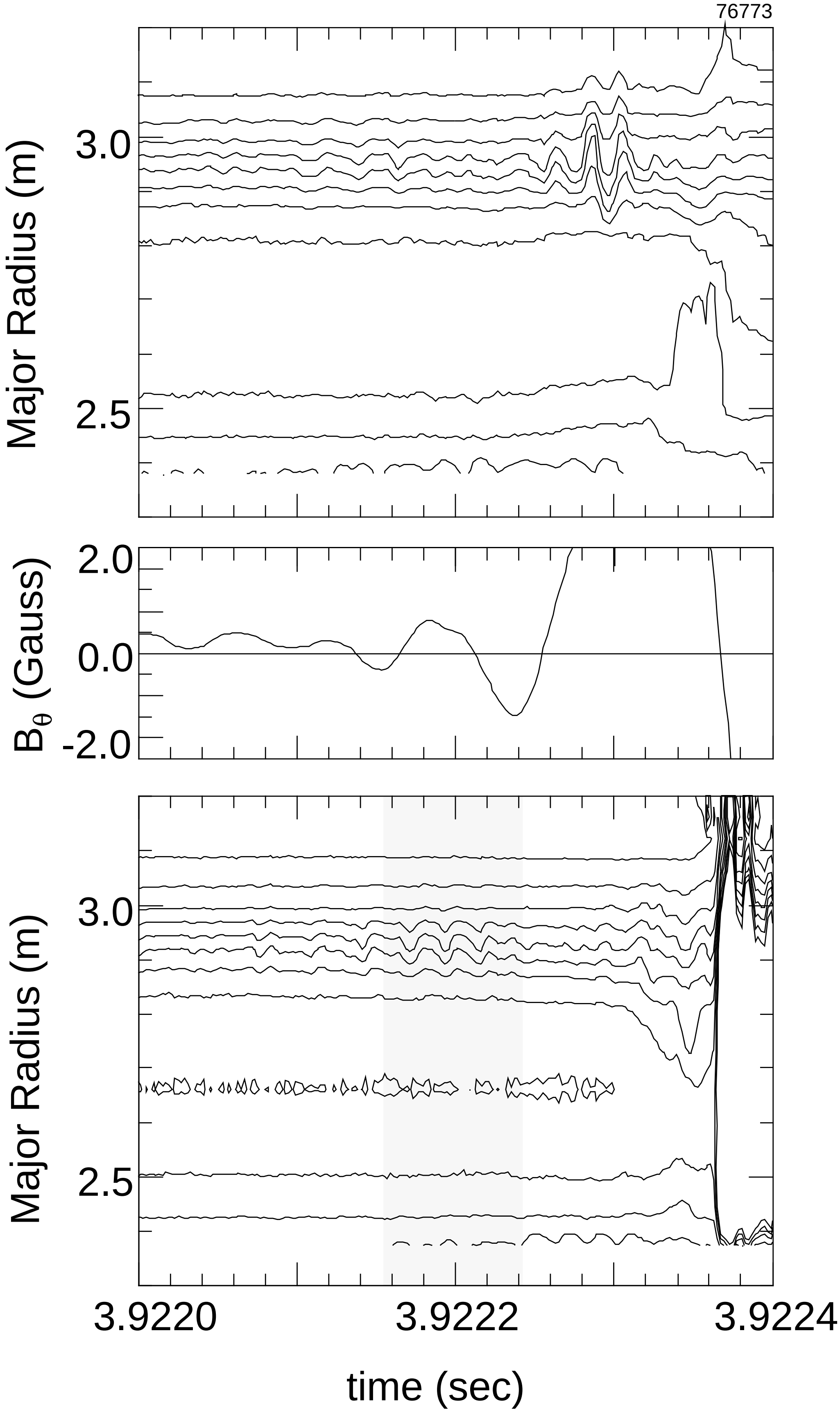

76773
Major Radius (m)
3.0
2.5
B_θ (Gauss)
2.0
0.0
-2.0
Major Radius (m)
3.0
2.5
3.9220
3.9222
3.9224
time (sec)

Figure 4

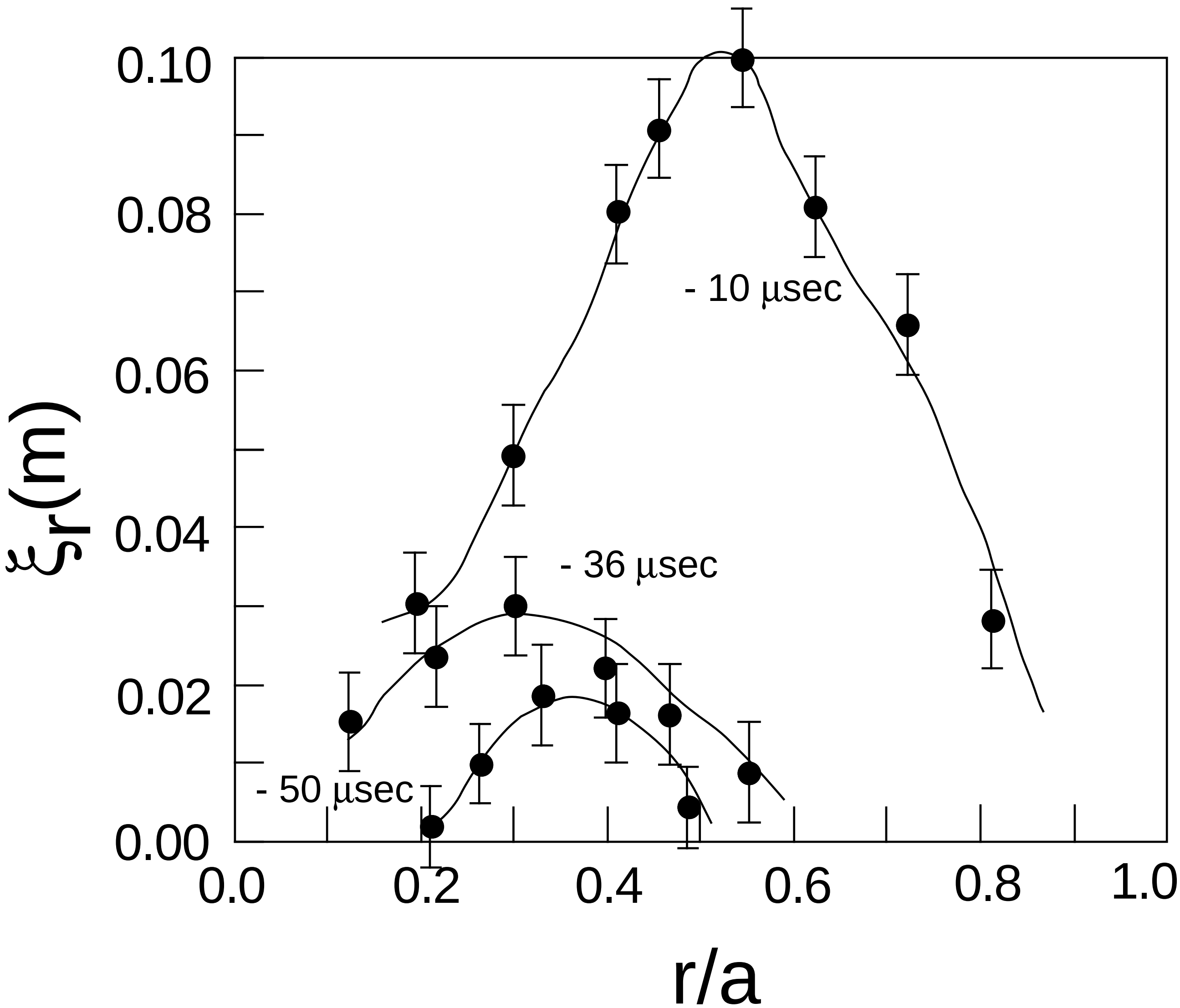
0.10
0.08
0.06
0.04
0.02
0.00
ξr(m)
- 10 μsec
- 36 μsec
- 50 μsec
0.0
0.2
0.4
0.6
0.8
1.0
r/a

Figure 5

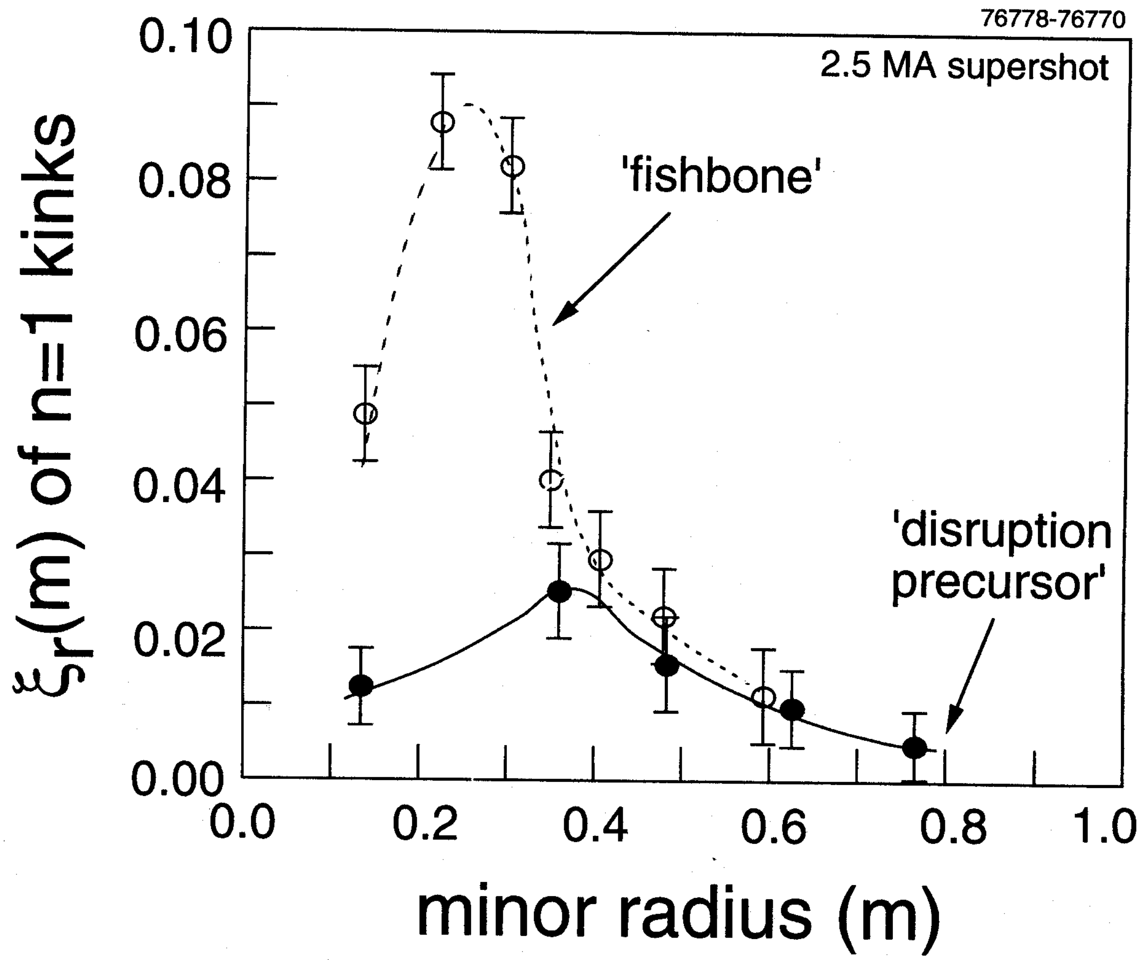
76778-76770
2.5 MA supershot
'fishbone'
'disruption precursor'
0.10
0.08
0.06
0.04
0.02
0.00
0.0
0.2
0.4
0.6
0.8
1.0
ξr(m) of n=1 kinks
minor radius (m)

Figure 6

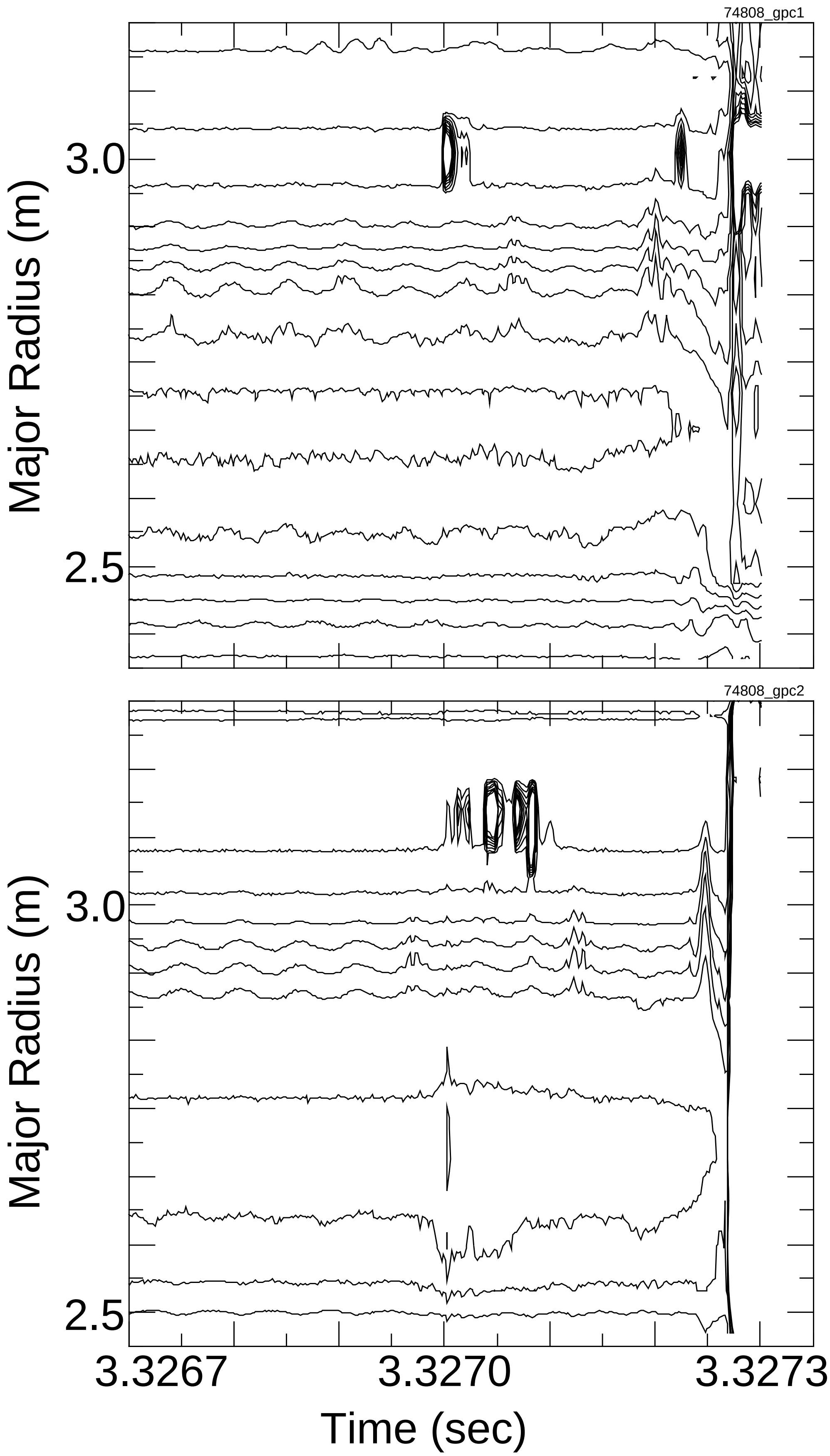
74808_gpc1
74808_gpc2
Major Radius (m)
3.0
2.5
Major Radius (m)
3.0
2.5
3.3267
3.3270
3.3273
Time (sec)